



# Density and morphology of coronary artery calcium for the prediction of cardiovascular events: insights from the Framingham Heart Study

Borek Foldyna<sup>1,2</sup> · Parastou Eslami<sup>1</sup> · Jan-Erik Scholtz<sup>1,3</sup> · Kristin Baltrusaitis<sup>4</sup> · Michael T. Lu<sup>1</sup> · Joseph M. Massaro<sup>4</sup> · Ralph B. D'Agostino Sr<sup>4</sup> · Maros Ferencik<sup>1,5</sup> · Hugo J. W. L. Aerts<sup>2,6</sup> · Christopher J. O'Donnell<sup>7,8</sup> · Udo Hoffmann<sup>1</sup>

Received: 24 January 2019 / Revised: 1 April 2019 / Accepted: 4 April 2019 / Published online: 2 May 2019

© European Society of Radiology 2019

## Abstract

**Objectives** To investigate the association between directly measured density and morphology of coronary artery calcium (CAC) with cardiovascular disease (CVD) events, using computed tomography (CT).

**Methods** Framingham Heart Study (FHS) participants with CAC in noncontrast cardiac CT (2002–2005) were included and followed until 2016. Participants with known CVD or uninterpretable CT scans were excluded. We assessed and correlated (Spearman) CAC density, CAC volume, and the number of calcified segments. Moreover, we counted morphology features including shape (cylindrical, spherical, semi-tubular, and spotty), location (bifurcation, facing pericardium, or facing myocardium), and boundary regularity. In multivariate Cox regression analyses, we associated all CAC characteristics with CVD events (CVD-death, myocardial infarction, stroke).

**Results** Among 1330 included participants ( $57.8 \pm 11.7$  years; 63% male), 73 (5.5%) experienced CVD events in a median follow-up of 9.1 (7.8–10.1) years. CAC density correlated strongly with CAC volume (Spearman's  $\rho = 0.75$ ;  $p < 0.001$ ) and lower number of calcified segments ( $\rho = -0.86$ ;  $p < 0.001$ ; controlled for CAC volume). In the survival analysis, CAC density was associated with CVD events independent of Framingham risk score (HR (per SD) = 2.09; 95%CI, 1.30–3.34;  $p = 0.002$ ) but not after adjustment for CAC volume ( $p = 0.648$ ). The extent of spherically shaped and pericardially sided calcifications was associated with fewer CVD events accounting for the number of calcified segments (HR (per count) = 0.55; 95%CI, 0.31–0.98;  $p = 0.042$  and HR = 0.66; 95%CI, 0.45–0.98;  $p = 0.039$ , respectively).

**Conclusions** Directly measured CAC density does not predict CVD events due to the strong correlation with CAC volume. The spherical shape and pericardial-sided location of CAC are associated with fewer CVD events and may represent morphological features related to stable coronary plaques.

## Key Points

- Coronary calcium density may not be independently associated with cardiovascular events.
- Coronary calcium density correlates strongly with calcium volume.
- Spherical shape and pericardial-sided location of CAC are associated with fewer CVD events.

**Electronic supplementary material** The online version of this article (<https://doi.org/10.1007/s00330-019-06223-7>) contains supplementary material, which is available to authorized users.

✉ Borek Foldyna  
bfoldyna@mgh.harvard.edu

<sup>1</sup> Cardiac MR PET CT Program, Massachusetts General Hospital, Harvard Medical School, 165 Cambridge Street, Suite 400, Boston, MA 02114, USA

<sup>2</sup> Radiology and Nuclear Medicine, CARIM, Maastricht University Medical Centre, Maastricht, Netherlands

<sup>3</sup> Department of Diagnostic and Interventional Radiology, University Hospital Frankfurt, Frankfurt, Germany

<sup>4</sup> Department of Mathematics, Boston University, Boston, MA, USA

<sup>5</sup> Knight Cardiovascular Institute, Oregon Health and Science University, Portland, OR, USA

<sup>6</sup> Dana-Farber Cancer Institute, Brigham and Women's Hospital, Harvard Medical School, Boston, MA, USA

<sup>7</sup> The Framingham Heart Study of the National Heart, Lung, and Blood Institute, Framingham, MA, USA

<sup>8</sup> Cardiology Section, VA Boston Healthcare System, West Roxbury, MA, USA

**Keywords** Multi-detector computed tomography · Coronary artery calcium · Coronary artery disease · Atherosclerosis · Cardiovascular system

### Abbreviations

AS	Agatston score
AUC	Area under the curve
BMI	Body mass index
CAC	Coronary artery calcium
CT	Computed tomography
CVD	Cardiovascular disease
FHS	Framingham Heart Study
FRS	Framingham risk score
HU	Hounsfield units
ICC	Intra-class correlation coefficient
IVUS	Intravascular ultrasound
LAD	Left anterior descending
LCx	Left circumflex artery
MESA	Multi-Ethnic Study of Atherosclerosis
RCA	Right coronary artery
VIF	Variance inflation factor

### Introduction

Coronary artery calcium (CAC) develops during the process of atherogenesis [1] and has a high prognostic value in symptomatic and asymptomatic individuals [2]. Traditional Agatston score (AS), derived from noncontrast computed tomography (CT) images, represents a clinical standard for CAC assessment [3]. Even though the traditional AS accounts for the CAC density (as a peak density factor), two investigations have suggested an inverse relationship between CAC density and cardiovascular disease (CVD) events independent of CAC volume [4, 5]; results of which could be reproduced by another study only in men [6]. However, these studies used an indirect measure of CAC density, calculated from the per-person AS and averaged across each patient as a substitute for direct density measurements. Results of CAC density measured directly and on the per-segment level are missing, and the association between CAC density, CAC volume, the number of calcified segments, and CVD events is unknown.

Moreover, CT images offer a high amount of information beyond volume and density. For instance, CAC may present with a broad spectrum of shapes and can appear at various locations and its boundaries can be regular or highly irregular [1, 7]. As suggested in smaller histopathological, biomechanical, and intravascular ultrasound (IVUS) studies, these characteristics may have a high prognostic value. For example in biomechanical models, unlike round calcifications, irregular configuration and oval shape with sharp edges have been associated with increased biomechanical stress on the surrounding tissue, representing a risk factor for plaque rupture [8].

Spotty CAC has been linked to inflammation, decreased plaque stability, and culprit lesions in patients with acute coronary syndrome [9, 10]. Furthermore, an *ex vivo* study, exploring coronary artery flow patterns, has shown that coronary plaques develop predominantly at bifurcations and along inner walls of curved coronary segments, potentially as a result of altered endothelial shear stress [11, 12].

Hence, we sought to investigate the association of directly CT-derived CAC density and morphology with CVD events.

### Materials and methods

#### Study population

The Framingham multi-detector CT sub-study included 4095 adults (men  $\geq 35$  and women  $\geq 40$  years of age) from the Offspring and Third Generation cohorts of the community-based Framingham Heart Study (FHS) [13]. For the current analysis, we included subjects with CAC on noncontrast cardiac CT (CAC  $> 0$ ), and complete risk profile. Participants with known CVD, missing or not readable scans were omitted. The institutional review boards of the Boston University Medical Center and Massachusetts General Hospital approved the study, and all participants provided written consent.

#### CVD events

Major CVD events were defined as death from coronary heart disease, non-fatal myocardial infarction, or ischemic stroke, according to the FHS [14] and the 2013 American College of Cardiology/American Heart Association risk assessment guidelines [15]. CVD events were adjudicated using medical histories, physical examinations at the study clinic, hospitalization records, and communication with personal physicians.

#### CT image acquisition and analysis

All participants underwent noncontrast ECG-triggered cardiac CT (2002–2005) using an eight-slice multi-detector CT scanner (LightSpeed Ultra; General Electric) (120 kVp, 320 or 400 mA for  $< 100$  and  $\geq 100$  kg of body weight, respectively; gantry rotation time, 500 ms). The imaging protocol included prospectively ECG-triggered sequential data acquisition initiated at 50% of the RR interval. All scans were performed in a single breath hold in mid-inspiration, and the images were reconstructed at 2.5-mm slice thickness and 350-mm field of view [13]. Three independent readers (BF, PE, JES)

segmented the CAC on a per-segment basis using an open-source workstation (3DSlicer, v.4.7.0, <http://www.slicer.org>) [16]. The major coronary vessels were divided into eight segments: (1) proximal and (2) distal right coronary artery (RCA), (3) left main, (4) proximal and (5) distal left anterior descending (LAD), (6) proximal and (7) distal circumflex artery (LCx), and (8) ramus intermedius. Following other studies, only  $\geq 3$  connected voxels with radiodensity  $> 130$  Hounsfield units (HU) were considered as CAC [3, 13]. We assigned calcifications which exceeded segment borders to the proximal segment of origin and excluded aortic calcifications which reached into the coronary ostia.

### Quantitative CAC measures—density, volume, and AS

The CAC density was directly measured in each calcification, defined as the highest radiodensity (HU) within a given segment. CAC volume ( $\text{mm}^3$ ) represented the sum of all calcified voxels within a given calcified segment. To obtain values per participant, we averaged all per-segment densities and summed the per-segment volumes. We also recorded the number of calcified segments (potential range 1–8) and the standard AS in every individual [3].

### Morphological features

We selected CAC morphology features including shape, location, and regularity of boundaries based on prior reports [7–12]. We determined the prevalence and extent of these features within a given individual by visual evaluation of the transversal CT images. Due to a low spatial resolution in the *z*-direction (clinical standard of 2.5 mm), microcalcifications and the regularity of boundaries were assessed exclusively in the transversal image with a higher spatial resolution of 0.4–0.6 mm. All other features were confirmed in sagittal and coronal multi-planar reconstructions. Supplemental Figure 1S provides corresponding image examples. Briefly, CAC shape included four major and not mutually exclusive categories: (1) cylindrical = tube-like calcification  $> 3$  mm, affecting the entire vessel circumference; (2) spherical = single, round lesion  $> 3$  mm; (3) semi-tubular = lumpy calcification  $> 3$  mm size, affecting only part of the vessel circumference and presenting with luminal convexity; (4) spotty = multiple small calcifications  $< 3$  mm size.

Regarding the location, we recorded the presence of calcified bifurcations (vessels  $> 2$  mm diameter) and assessed the location of CAC within the vessel (facing pericardium, myocardium, or both). The regularity of boundaries reflected the quality of the CAC edges. Homogeneously smooth edges were rated as regular, while inhomogeneous or not differentiable edges as irregular.

### Inter-software and inter-/intra-observer reliability

The AS, obtained by 3DSlicer, revealed an excellent inter-software/inter-reader agreement with the AS acquired in the initial analysis using commercially available software (intra-class correlation coefficient (ICC) = 0.98) [13]. There was a substantial agreement between all three readers regarding the identification of the morphological features with Cohen's kappa values ranging from 0.52 to 1.0 (Supplemental Table 1S).

### Statistical analysis

Continuous variables were expressed as mean  $\pm$  standard deviation (SD) or median (inter-quartile range), and categorical variables as frequencies and percentages. Skewed variables were *natural log*-transformed. First, we assessed the relationship between CAC density, volume, AS, and the number of calcified segments using Spearman correlations ( $\rho = \text{rho}$ ). We categorized the CAC density into quartiles and listed the event rates in individual groups, enhanced by a Kaplan-Meier curves (incl. log-rank test). In univariate and multivariate Cox regressions, we investigated the predictive value of CAC density adjusting stepwise for the FRS and CAC volume. In a supplemental analysis, all regressions were repeated in subgroups stratified by sex and the use of statins.

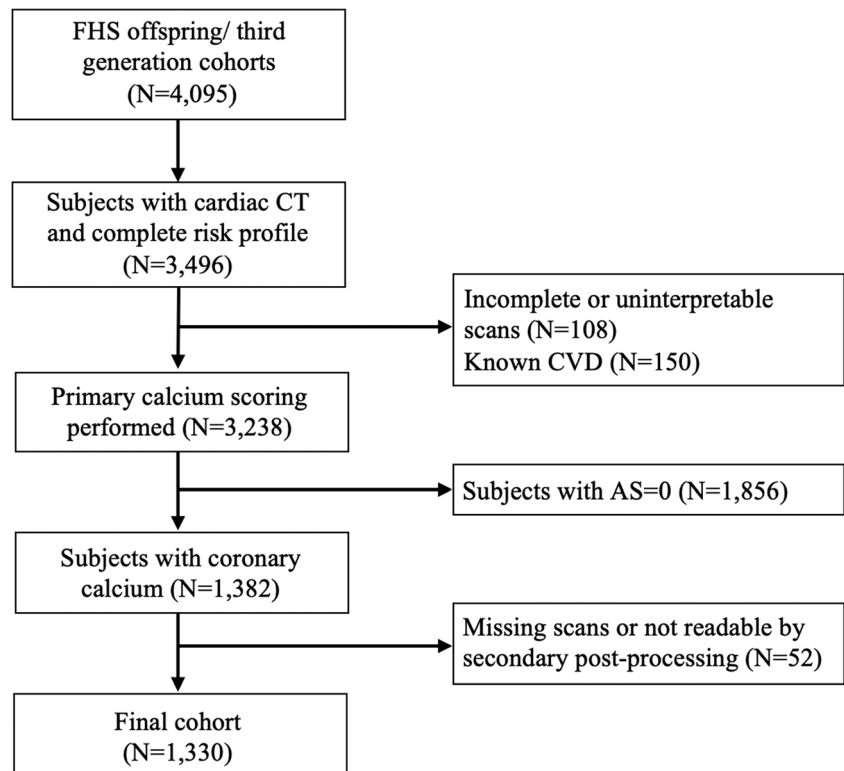
Second, we compared the prevalence of the individual morphological features between groups with and without CVD events using Fisher's exact test, enhanced by Kaplan-Meier curves (incl. log-rank tests). After ruling out collinearity between the morphological features (variance inflation factor (VIF)  $< 4$  for no-collinearity), we associated the extent of the features with CVD events using univariate and multivariate Cox regressions. To account for the extent of CAD, we adjusted the multivariate Cox regressions for the number of calcified segments. We did not adjust for the overall CAC volume, since the qualitative morphological features did not include information about the size of individual calcifications; this aspect was investigated in the density part of our manuscript. Two-sided  $p < 0.05$  was considered as statistically significant, and Stata 14.0 (StataCorp LP) was used for all analyses.

## Results

### Participant demographics

Among the 4095 CT sub-study participants, 1330 (838 (63%) males; mean age  $57.8 \pm 11.7$  years) presented with CAC in the cardiac CT scan, had a complete risk profile, and had no history of CAD (Fig. 1). Overall, 73 (5.5%) subjects experienced CVD events during the median follow-up of 9.1 (7.8–10.1) years. These individuals presented with higher cardiovascular risk at baseline (FRS,  $14.2 \pm 9.2\%$  vs.  $9.3 \pm 6.7\%$ ;  $p < 0.001$ ) (Table 1).

**Fig. 1** Consort diagram. AS, Agatston score; CVD, cardiovascular disease; CT, computed tomography



### CAC density, CAC volume, AS, and the number of calcified segments

Overall, the median CAC density was 364.0 (230.0–526.0) HU, while the CAC volume, AS, and the number of calcified segments per person were 364.0 (230.0–526.0) mm<sup>3</sup>, 60.2 (10.1–228.5), and 3 (1–4), respectively. On the per-person level, CAC density correlated strongly with CAC volume and AS (Spearman's  $\rho = 0.75$  and  $\rho = 0.82$ ;  $p < 0.001$  for both) while less with the number of calcified segments ( $\rho = 0.40$ ;  $p < 0.001$ ). Moreover, lower CAC density correlated strongly with higher number of calcified segments after adjustment for CAC volume ( $\rho = -0.86$ ;  $p < 0.001$ ), suggesting that the mean density per person decreased with an increasing number of calcifications at a given CAC volume. On the per-segment level, the median CAC density of individual lesions (357.5 (201.0–606.5) HU) correlated strongly with the median lesion size (25.7 (8.2–75.9) mm<sup>3</sup>) ( $\rho = 0.86$ ;  $p < 0.001$ ). Figure 2 provides corresponding scatter plots.

### Association of CAC density with CVD events

In the univariate analysis, participants with CVD events had ~30% higher CAC density as compared with those without events (464.0 (352.8–606.0) vs. 356.0 (226.0–517.3) HU;  $p < 0.001$  for difference) (Table 2). The event rate increased proportionally across quartiles of CAC density; also reflected in a lower event-free survival in participants with higher CAC

density (Fig. 3). Higher CAC density was related to a lower event-free survival in both women and men (log-rank:  $p \leq 0.004$ ; Supplemental Figure 2S).

In the unadjusted survival analysis, CAC density, CAC volume, AS, and the number of calcified segments were associated with CVD events (HR = 1.44–2.59;  $p < 0.001$  for all) and remained significant after accounting for FRS (HR = 1.33–2.09;  $p < 0.001$ –0.002). However, the association of CAC density with CVD events was attenuated after adjustment for CAC volume (HR = 0.84; 95%CI, 0.41–1.74;  $p = 0.648$ ) (Table 3). Similar results were found in the subgroup analysis stratified by sex and statin use ( $p = 0.138$ –875 for CAC volume-adjusted models) (Supplemental Table 2S).

### Morphological CAC features and CVD events

The prevalence of the morphological features ranged between 10.5 and 89.9%, while the extent ranged between 1.3 and 2.4 (mean) features per participant (Supplemental Table 3S). The prevalence of cylindrical and semi-tubular shapes, calcified bifurcations, both-sided lesions, and irregular boundaries was twice as high in the participant group with CVD events compared with the others ( $p < 0.001$ –0.005), also reflected in a lower event-free survival (log-rank  $p < 0.001$ –0.004) (Supplemental Figure 3S). In the survival analysis adjusted for the number of calcified segments, spherical shape and pericardial-sided CAC were associated with less CVD events

**Table 1** Baseline characteristics stratified by CVD events

	All (N=1330)	No CVD (N=1257)	CVD (N=73)	p
Age (years)	57.8 ± 11.7	57.4 ± 11.7	64.5 ± 10.7	<0.001
Men, N (%)	838 (63.0)	791 (62.9)	47 (64.4)	0.901
On statin treatment, N (%)	240 (18.0)	228 (18.1)	12 (16.4)	0.876
Cardiovascular risk factors				
Total cholesterol (mg/dl)	201.7 ± 34.8	201.6 ± 35.0	201.5 ± 33.5	0.982
HDL cholesterol (mg/dl)	50.9 ± 15.7	51.2 ± 15.7	46.6 ± 14.2	0.011
Triglycerides (mg/dl)	143.3 ± 101.4	142.5 ± 101.7	155.6 ± 95.5	0.040
Hypertension, N (%)	531 (39.9)	495 (39.4)	36 (49.3)	0.110
Hypertensive treatment, N (%)	342 (25.7)	317 (25.2)	25 (34.2)	0.098
Systolic blood pressure (mmHg)	126.6 ± 16.8	126.2 ± 16.8	133.0 ± 16.7	0.001
Diastolic blood pressure (mmHg)	77.1 ± 9.5	77.1 ± 9.5	75.7 ± 9.5	0.103
Diabetes mellitus, N (%)	117 (8.8)	105 (8.4)	12 (16.4)	0.022
BMI (kg/m <sup>2</sup> )	28.8 ± 5.1	28.7 ± 5.1	29.5 ± 5.4	0.178
Current smoker, N (%)	171 (12.9)	158 (12.6)	13 (17.8)	0.133
FRS (%)	10.0 ± 0.7	9.3 ± 6.7	14.2 ± 9.2	<0.001

All values are displayed as means ± SD or N (%). p values are based on Wilcoxon rank-sum or Fisher's exact tests as appropriate. BMI, body mass index; CVD, cardiovascular disease; FRS, Framingham risk score; HDL, high-density lipoprotein

(HR (per count) = 0.55; 95%CI, 0.31–0.98; p = 0.042 and HR = 0.66; 95%CI, 0.45–0.98; p = 0.039) (Table 4).

## Discussion

We assessed the relationship between the directly measured CAC density, CAC volume, number of calcified coronary segments, and CVD events in 1330 participants of the

community-based FHS using noncontrast cardiac CT. Moreover, we investigated the association of 10 morphological CAC features with CVD events; features which have been described previously in CT, IVUS and histology studies as well as in biomechanical models. Our results suggest that the directly measured CAC density correlates strongly with CAC volume on the per-person and per-segment levels and that with an increasing number of calcified segments, CAC density decreases at any level of CAC volume. CAC density

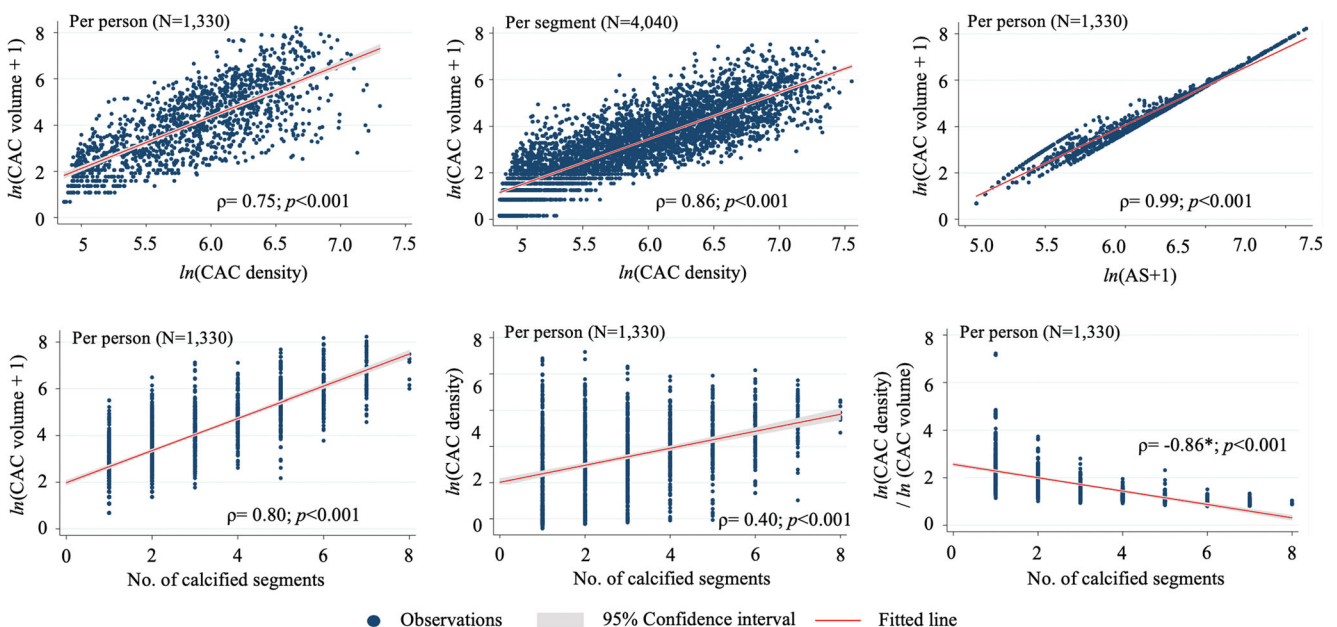


**Fig. 2** Correlation between CAC density, CAC volume, AS, and number of calcified segments. CAC density revealed a strong correlation with measures of CAC quantity. The proportion of CAC density/volume

decreased with increasing number of calcified segments. \*Partial correlation between CAC density and No. of calcified segments. CAC, coronary artery calcification

**Table 2** Absolute measures of CAC stratified by CVD events

	All (N= 1330)	No CVD (N= 1257)	CVD (N= 73)	p
CAC density (HU)	364.0 (230.0–526.0)	356.0 (226.0–517.3)	464.0 (352.8–606.0)	< 0.001
CAC volume (mm <sup>3</sup> )	53.5 (15.6–186.0)	50.6 (14.6–175.2)	232.7 (120.7–444.9)	< 0.001
Agatston score	60.2 (10.1–228.5)	55.8 (9.7–209.0)	284.3 (137.3–593.2)	< 0.001
No. of calcified segments	3 (1–4)	3 (1–4)	4 (3–6)	< 0.001

Individuals with CVD events had higher median CAC density and a greater amount of CAC (volume, AS, and calcified segments). All values are displayed as median (inter-quartile range). *p* values are based on Wilcoxon rank-sum or Fisher’s exact tests as appropriate. *CAC*, coronary artery calcium; *HU*, Hounsfield units

was a predictor of CVD events independent of traditional cardiovascular risk but was not independent of CAC volume. The extent of spherically shaped and pericardially sided calcifications was associated with fewer CVD events accounting for the number of calcified segments and, thus, may represent morphological features related to stable coronary plaques.

### CAC density

In general, there are three primary concepts which have emerged in the evaluation of CAC: assessment of (i) quantity, (ii) distribution, and (iii) density. The quantity of CAC, traditionally measured not only by AS but also by CAC volume or the number of calcified segments, reflects the individual burden of atherosclerosis and is a well-known marker of CVD risk [17–19]. Our results are in line with the prior studies and demonstrate that CAC quantity is a strong predictor of CVD events independent of traditional cardiovascular risk factors. Despite the strong predictive value of CAC quantity, the number of coronary arteries affected by CAC relative to CAC volume [20–22] and the presence of CAC in the proximal dominant coronary artery [22] have been related to CVD events independent of CAC volume and traditional cardiovascular risk factors. These factors underline the importance of CAC distribution and location within a given individual. We

deliver novel data which show that CAC volume, density, and distribution are strongly related.

Regarding the concept of density, most of the published studies are limited to the CAC density factor, calculated from the overall per-person Agatston score [4]. Using the calculated CAC density factor, two publications have associated a low density with CVD events at any level of CAC volume [4, 5]. The association between low CAC density and events appears intuitively correct as one could imagine that lower density may reflect a more mixed nature of the given lesion with an underlying noncalcified plaque that is just not visible in noncontrast CT, both due to the lack of contrast and due to the lower spatial resolution of noncontrast cardiac scans.

Despite a much larger study population (N= 63,215), Shaw et al could reproduce these results only in men but not in women [6]. A smaller study in hemodialysis patients has suggested the opposite, namely the association of high density with increased all-cause mortality [23], and another recent study in patients with advanced chronic kidney disease has described the highest risk of mortality in patients with intermediate CAC density (i.e., mid tertile; inverted J-shaped relation) [24].

Since calculated from the overall AS per-person, the CAC density factor inevitably does not account for the distribution of calcifications within a given individual. Nevertheless, Blaha et al reported that higher diffusivity index, as a marker

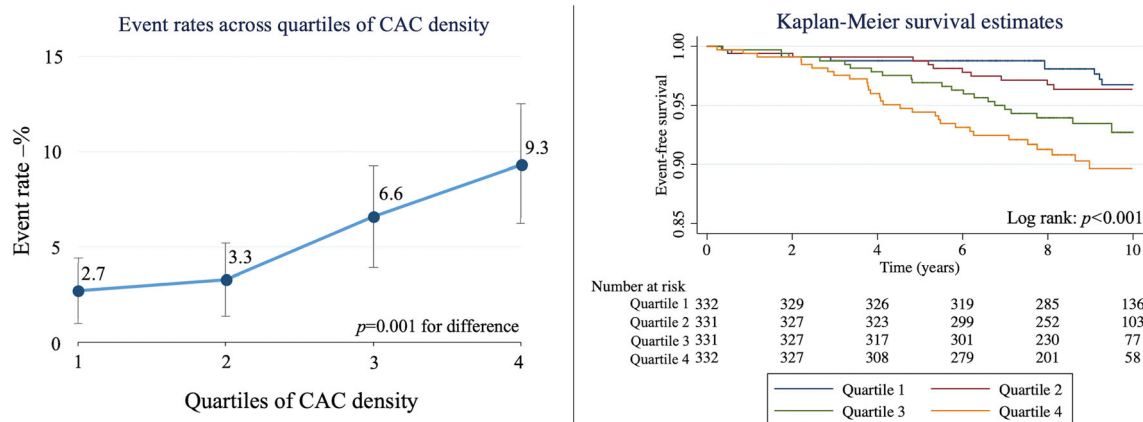


**Fig. 3** Event rates across quartiles of CAC density and corresponding Kaplan-Meier estimates. Higher event rates and lower event-free survival in the higher quartiles of CAC density. Whiskers represent 95% confidence intervals. *CAC*, coronary artery calcium

**Table 3** Association of CAC density and volume with CVD events

	Univariate			Multivariate					
	HR	95%CI	<i>p</i>	Adjustment: FRS			Adjustment: FRS + ln (CAC volume + 1)		
				HR	95%CI	<i>p</i>	HR	95%CI	<i>p</i>
ln (CAC density)	2.59	1.65–4.06	<0.001	2.09	1.30–3.34	0.002	0.84	0.41–1.74	0.648
ln (CAC volume + 1)	1.60	1.38–1.86	<0.001	1.46	1.25–1.72	<0.001	–	–	–
ln (AS + 1)	1.51	1.33–1.73	<0.001	1.40	1.21–1.61	<0.001	1.43	0.53–3.89	0.478
No. of calcified segments	1.44	1.28–1.62	<0.001	1.33	1.17–1.51	<0.001	1.12	0.92–1.37	0.266

Univariate and multivariate Cox regressions to associate the quantitative CAC features with CVD events. AS, Agatston score; CAC, coronary artery calcium; FRS, Framingham risk score

of broader CAC distribution and more diffuse atherosclerosis, relates to a higher risk of events at any level of AS [20]. Thus, for instance, a person with multiple small calcifications and a given AS is at higher CVD risk than a person with the same AS but one large calcification. Accordingly, the CAC density factor would be the same in both individuals and would not reflect differences in cardiovascular risk potentially driven by differences of CAC distribution.

Our results underscore this issue by showing that the directly measured CAC density correlates strongly with CAC volume on per-patient level ( $\rho = 0.75$ ) and on per-segment level ( $\rho = 0.86$ ). The strong collinearity between volume and density may explain why the initially strong positive association between CAC density and CVD events vanished after adjustment for CAC volume. Moreover, lower CAC density

correlated with higher number of calcified segments ( $\rho = -0.86$ ) at any level of CAC volume. In other words, smaller calcifications had lower density independent of CAC burden. This finding is not surprising, considering that the median size of individual calcifications is small (26 mm<sup>3</sup>; ~equivalent to 3 × 3 × 3 mm) and the usual CT slice thickness is high (usually 2.5–3 mm). Thus, partial volume effect may influence the CAC density, and a broader CAC distribution (i.e., smaller calcifications) may lower and confound the per-person CAC density factor. Therefore, rather than conflict prior studies [4–6, 23, 24], our results enhance the knowledge by showing a close relationship between the directly measured CAC density, volume, and distribution.

Future studies should ideally measure the CAC density directly at the segmental level and acknowledge the CAC

**Table 4** Association of morphological CAC features with CVD events

	Univariate			Multivariate Adjustment: Number of calcified segments		
	HR	95%CI	<i>p</i>	HR	95%CI	<i>p</i>
<b>Shape</b>						
Cylindrical	1.71	1.25–2.33	0.001	1.15	0.81–1.62	0.424
Spherical	0.62	0.34–1.12	0.115	0.55	0.31–0.98	0.042
Semi-tubular	1.49	1.31–1.68	<0.001	1.19	0.99–1.44	0.067
Spotty	1.30	1.15–1.47	<0.001	0.89	0.74–1.06	0.182
<b>Location</b>						
Bifurcations	1.31	1.11–1.55	0.001	0.87	0.67–1.09	0.233
Myocardial side	0.95	0.69–1.32	0.774	0.82	0.60–1.12	0.217
Pericardial side	0.71	0.47–1.07	0.103	0.66	0.45–0.98	0.039
Both-sided	1.40	1.24–1.57	<0.001	1.07	0.90–1.28	0.456
<b>Regularity of boundaries</b>						
Regular	1.13	0.93–1.37	0.209	0.93	0.78–1.10	0.408
Irregular	1.36	1.20–1.55	<0.001	1.03	0.87–1.22	0.752

Univariate and multivariate Cox regressions to associate the extent of individual features per subject (range 0–8) with CVD events

distribution. Studies using the calculated CAC density factor should adjust for CAC distribution (e.g., diffusivity index [20]).

## CAC morphology

CAC morphology represents a novel concept to assess CAC. Studies of biomechanical models have suggested that the shape of CAC may be associated with mechanical stress on the surrounding tissue and, thus, that sharp edges and irregular shapes of CAC may lead to a reduced the stability of atherosclerotic plaque caps [8]. Our findings support these observations by showing that spherical calcifications (i.e., less mechanical stress) are associated with fewer CVD events after adjustment for the number of calcified segments (HR = 0.55). Furthermore, pericardial-sided calcifications were less prevalent than myocardial-sided lesions and were associated with fewer CVD events adjusted for the number of calcified segments (HR = 0.66). These observations support histological, angiography, and IVUS studies as well as swine models suggesting an accelerated plaque development in inner side of curved coronary segments (i.e., myocardial side) induced by lower blood flow and reduced endothelial shear stress [11, 12, 25]. Future studies focusing on CAC shape and location in culprit lesions are needed to render features with a predictive value potentially related to high-risk plaques.

## Study limitations

The number of CVD events was relatively low in this study which may have influenced the power of our study; however, we included only hard CVD events (i.e., cardiovascular death, non-fatal myocardial infarction, ischemic stroke). On the technical side, the exact determination of coronary segments in noncontrast CT scans can sometimes be difficult, and thus, we reduced the number of segments from 18 to 8. This adjustment may decline the comparability with other studies applying the standard 18-segment model. Lastly, the CT images were acquired and reconstructed with standard clinical methods. Thus, the image resolution in the z-direction was low (2.5 mm), did lead to a higher partial volume effect, and may have influenced the evaluation of the morphological CAC features. Future studies using images with spatial resolution higher than the current clinical standard are desirable.

## Conclusions

Directly measured CAC density is not a predictor of CVD events independent of CAC volume. The directly measured CAC density correlates strongly with the CAC volume on the per-person and per-segment levels and decreases with increasing number of calcified segments at a given CAC volume. The spherical shape and pericardial-sided location of CAC are

associated with fewer CVD events and may represent morphological features related to stable coronary plaques.

**Acknowledgments** This study used in part data and resources from the Framingham Heart Study of the National Heart, Lung, and Blood Institute of the National Institutes of Health and Boston University School of Medicine. Dr. Borek Foldyna, Dr. Udo Hoffmann, and Dr. Christopher J. O'Donnell have had full access to all the study data and take responsibility for the data integrity and the analysis accuracy.

Our project was presented at the SCCT 2018 in Dallas, TX, USA, and received the Siemens Outstanding Academic Research (SOAR) award.

**Funding** The authors state that this work has not received any funding.

## Compliance with ethical standards

**Conflict of interest** Dr. Foldyna received unrelated funding from the German Research Foundation (DFG), project 290004377 (FO993/1) and support from the National Institutes of Health 5K24HL113128-07. Dr. Hoffmann received unrelated Research Grants (U01HL092040, U01HL092022, Heart Flow Inc., MedImmune; KOWA Inc.). Dr. Ferencik reports receiving an unrelated grant from the American Heart Association. This work was further supported by the NIH Heart, Lung, and Blood Institute's Framingham Heart Study (contract nos. N01-HC-25195, HL076784, AG028321, HL070100, HL060040, HL080124, HL071039, HL077447, HL107385). The authors of this manuscript declare no relationships with any companies, whose products or services may be related to the subject matter of the article.

**Study subjects or cohorts overlap** Some study subjects or cohorts have been previously reported in the scope of prior Framingham Heart Study investigations.

This study used in part data and resources from the Framingham Heart Study of the National Heart, Lung, and Blood Institute of the National Institutes of Health and Boston University School of Medicine. Dr. Borek Foldyna, Dr. Udo Hoffmann, and Dr. Christopher J. O'Donnell have had full access to all the study data and take responsibility for the data integrity and the analysis accuracy.

## Methodology

- retrospective
- observational
- performed at one institution (study center)

## References

1. Nakahara T, Dweck MR, Narula N et al (2017) Coronary artery calcification: from mechanism to molecular imaging. *JACC Cardiovasc Imaging* 10:582–593. <https://doi.org/10.1016/j.jcmg.2017.03.005>
2. Nasir K, Clouse M (2012) Role of nonenhanced multidetector CT coronary artery calcium testing in asymptomatic and symptomatic individuals. *Radiology* 264:637–649. <https://doi.org/10.1148/radiol.12110810>
3. Agatston AS, Janowitz WR, Hildner FJ, Zusmer NR, Viamonte M Jr, Detrano R (1990) Quantification of coronary artery calcium using ultrafast computed tomography. *J Am Coll Cardiol* 15:827–832
4. Criqui MH, Denenberg JO, Ix JH et al (2014) Calcium density of coronary artery plaque and risk of incident cardiovascular events. *JAMA* 311:271–278. <https://doi.org/10.1001/jama.2013.282535>



5. Criqui MH, Knox JB, Denenberg JO et al (2017) Coronary artery calcium volume and density. *JACC Cardiovasc Imaging* 10:845–854. <https://doi.org/10.1016/j.jcmg.2017.04.018>
6. Shaw LJ, Min JK, Nasir K et al (2018) Sex differences in calcified plaque and long-term cardiovascular mortality: observations from the CAC Consortium. *Eur Heart J* 39:3727–3735. <https://doi.org/10.1093/eurheartj/ehy534>
7. Lee JB, Mintz GS, Lissauskas JB et al (2011) Histopathologic validation of the intravascular ultrasound diagnosis of calcified coronary artery nodules. *Am J Cardiol* 108:1547–1551. <https://doi.org/10.1016/j.amjcard.2011.07.014>
8. Cardoso L, Kelly-Arnold A, Maldonado N, Laudier D, Weinbaum S (2014) Effect of tissue properties, shape and orientation of microcalcifications on vulnerable cap stability using different hyperelastic constitutive models. *J Biomech* 47:870–877. <https://doi.org/10.1016/j.jbiomech.2014.01.010>
9. Kataoka Y, Wolski K, Uno K et al (2012) Spotty calcification as a marker of accelerated progression of coronary atherosclerosis: insights from serial intravascular ultrasound. *J Am Coll Cardiol* 59:1592–1597. <https://doi.org/10.1016/j.jacc.2012.03.012>
10. Motoyama S, Kondo T, Sarai M et al (2007) Multislice computed tomographic characteristics of coronary lesions in acute coronary syndromes. *J Am Coll Cardiol* 50:319–326. <https://doi.org/10.1016/j.jacc.2007.03.044>
11. Asakura T, Karino T (1990) Flow patterns and spatial distribution of atherosclerotic lesions in human coronary arteries. *Circ Res* 66:1045–1066. <https://doi.org/10.1161/01.RES.66.4.1045>
12. Chatzizisis YS, Jonas M, Coskun AU et al (2008) Prediction of the localization of high-risk coronary atherosclerotic plaques on the basis of low endothelial shear stress: an intravascular ultrasound and histopathology natural history study. *Circulation* 117:993–1002. <https://doi.org/10.1161/CIRCULATIONAHA.107.695254>
13. Hoffmann U, Massaro JM, Fox CS, Manders E, O'Donnell CJ (2008) Defining normal distributions of coronary artery calcium in women and men (from the Framingham Heart Study). *Am J Cardiol* 102:1136–1141.e1. <https://doi.org/10.1016/j.amjcard.2008.06.038>
14. D'Agostino RB Sr, Vasan RS, Pencina MJ et al (2008) General cardiovascular risk profile for use in primary care: the Framingham Heart Study. *Circulation* 117:743–753. <https://doi.org/10.1161/CIRCULATIONAHA.107.699579>
15. Goff DC Jr, Lloyd-Jones DM, Bennett G et al (2014) 2013 ACC/AHA guideline on the assessment of cardiovascular risk: a report of the American College of Cardiology/American Heart Association Task Force on Practice Guidelines. *J Am Coll Cardiol* 63:2935–2959. <https://doi.org/10.1016/j.jacc.2013.11.005>
16. 3D Slicer. Available via <https://www.slicer.org/>. Accessed 16 Jun 2017
17. Detrano R, Guerci AD, Carr JJ et al (2008) Coronary calcium as a predictor of coronary events in four racial or ethnic groups. *N Engl J Med* 358:1336–1345. <https://doi.org/10.1056/NEJMoa072100>
18. Greenland P, LaBree L, Azen SP, Doherty TM, Detrano RC (2004) Coronary artery calcium score combined with Framingham score for risk prediction in asymptomatic individuals. *JAMA* 291:210–215. <https://doi.org/10.1001/jama.291.2.210>
19. Hoffmann U, Massaro JM, D'Agostino RB Sr, Kathiresan S, Fox CS, O'Donnell CJ (2016) Cardiovascular event prediction and risk reclassification by coronary, aortic, and valvular calcification in the Framingham Heart Study. *J Am Heart Assoc* 5. <https://doi.org/10.1161/JAHA.115.003144>
20. Blaha MJ, Budoff MJ, Tota-Maharaj R et al (2016) Improving the CAC score by addition of regional measures of calcium distribution: Multi-Ethnic Study of Atherosclerosis. *JACC Cardiovasc Imaging* 9:1407–1416. <https://doi.org/10.1016/j.jcmg.2016.03.001>
21. Brown ER, Kronmal RA, Bluemke DA et al (2008) Coronary calcium coverage score: determination, correlates, and predictive accuracy in the Multi-Ethnic Study of Atherosclerosis. *Radiology* 247:669–675. <https://doi.org/10.1148/radiol.2473071469>
22. Ferencik M, Pencina KM, Liu T et al (2017) Coronary artery calcium distribution is an independent predictor of incident major coronary heart disease events: results from the Framingham Heart Study. *Circ Cardiovasc Imaging* 10:e006592. <https://doi.org/10.1161/CIRCIMAGING.117.006592>
23. Bellasi A, Ferramosca E, Ratti C, Block G, Raggi P (2016) The density of calcified plaques and the volume of calcium predict mortality in hemodialysis patients. *Atherosclerosis* 250:166–171. <https://doi.org/10.1016/j.atherosclerosis.2016.03.034>
24. Mukai H, Dai L, Chen Z et al (2018) Inverse J-shaped relation between coronary arterial calcium density and mortality in advanced chronic kidney disease. *Nephrol Dial Transplant*. <https://doi.org/10.1093/ndt/gfy352>
25. Stone PH, Saito S, Takahashi S et al (2012) Prediction of progression of coronary artery disease and clinical outcomes using vascular profiling of endothelial shear stress and arterial plaque characteristics: the PREDICTION Study. *Circulation* 126(2):172–181. <https://doi.org/10.1161/CIRCULATIONAHA.112.096438>

**Publisher's note** Springer Nature remains neutral with regard to jurisdictional claims in published maps and institutional affiliations.